Scanning Tunneling Microscopic Investigation of 1T-MoS_2

F. Wypych,† Th. Weber, and R. Prins*

Laboratory for Technical Chemistry, Swiss Federal Institute of Technology (ETH), 8092 Zurich, Switzerland

Received June 4, 1997. Revised Manuscript Received December 18, 1997

The surface structure of the metastable solid-state compound 1T-MoS_2 was investigated by means of scanning tunneling microscopy (STM). In crystalline 1T-MoS_2, which is prepared by oxidation from the intercalation compound $K_x(H_2O)_yMoS_2$ ($x \approx 0.3$), every Mo center is octahedrally surrounded by six sulfur ligands, leading to an $a\sqrt{3} \times a\sqrt{3}$ surface structure. A similar MoS_2-type phase, but with a smaller amount of intercalated potassium ($x < 0.3$) and a different surface structure ($2a \times a$), forms under the same conditions at an earlier stage of the oxidation reaction. Comparison of the surface structures of these compounds revealed that this type of superstructure is determined not only by intrinsic properties, such as the degree of distortion within the [MoS_6] octahedra, but also by external factors. The latter lead to stabilization of the structural disorder, as does a film of water on the surface of the compounds. The surface structure of these compounds is, therefore, less characteristic than the bulk structure type as found in a thermodynamically stable solid. Upon heating in inert gas, rearrangement to the stable 2H-MoS_2 structure type takes place.

Introduction

Crystalline, amorphous, and intercalation compounds of MoS_2 show a variety of unusual structural, electronic, and optical properties. They are used as solid-state lubricants, as catalysts in hydrotreating reactions (crystalline and amorphous MoS_2-type compounds, respectively), and as cathode material in alkali metal batteries (MoS_2, MoS_3). Intercalation compounds of MoS_2 are of special interest because of their synthetic potential for the preparation of new modifications of MoS_2 as well as so-called nanocomposites in which organic macromolecules are located between the MoS_2 layers. A common property of all these Mo−S compounds is their behavior during thermal treatment, i.e., they are converted to 2H−MoS_2 which is the thermodynamically favored Mo^{IV}-S solid-state compound.

2H−MoS_2 is a semiconductor and consists of stacks of slabs, each of which is composed of two layers of sulfur atoms with a layer of molybdenum atoms between them. Every Mo center is coordinated to six sulfur ligands in a regular trigonal prismatic arrangement. The interaction between two neighboring MoS_2 slabs is rather weak and corresponds to van der Waals forces.[1]

Whereas 2H−MoS_2 has been known for a long time, the metastable 1T modification was discovered only a few years ago while investigating the above- mentioned intercalation compounds. 1T-MoS_2 has a distorted CdI_2-type structure and shows metallic behavior.[2] In the crystalline state all Mo centers are coordinated to six sulfur ligands in a distorted octahedral arrangement. The Mo centers are displaced from their ideal positions so that 3 Mo centers always come closer to each other (trimerization) and an $a\sqrt{3} \times a\sqrt{3}$ superstructure forms (a: lattice parameter of 2H−MoS_2). A detailed discussion can be found in ref 3. A schematic presentation of the 2H and 1T bulk structure types, with a regular trigonal prismatic and octahedral coordination of the metal centers, is shown in Figure 1. Note that the local coordination of Mo in 1T-MoS_2 is distorted octahedral, i.e., the Mo−S distances within the [MoS_6] octahedra are different. The 1T structure type in Figure 1, therefore, is an idealized presentation of the 1T-MoS_2 bulk structure.

1T-MoS_2 can be prepared by oxidation from the intercalation compound $K_x(H_2O)_yMoS_2$. In $K_x(H_2O)_y$-MoS_2, $x \approx 0.3$, hydrated K^+ cations are located between the MoS_2 layers. Due to distortions within the (a,b) plane, rows of sulfur atoms form along the b-axis[4] and lead to a monoclinic structure ($a \times a\sqrt{3}$ superstructure) as in the case of WTe_2.[5] A structural characterization of $K_x(H_2O)_yMoS_2$ by means of selected area electron diffraction (SAED) will be published elsewhere.[6]

Intercalation compounds of MoS_2 with lithium, Li_z-MoS_2, behave quite differently. The type of distortion in these compounds is mainly determined by the number of Li^+ cations present in octahedral and tetrahedral interstices in the van der Waals gaps[7] and can be adjusted by using different synthetic routes. Li_zMoS_2

* To whom correspondence should be addressed. Phone: + 41-1-632-5490. Fax: + 41-1-632-1162. E-mail: prins@tech.chem.ethz.ch.

† Permanent address: Universidade Federal do Paraná, CP 19081, 81531-990 Curitiba Pr, Brazil.

(1) Bronsema, K. D.; De Boer, J. L.; Jellinek, F. *Z. Anorg. Allg. Chem.* **1986**, *540/541*, 15.

(2) Wypych, F.; Schöllhorn, R. *J. Chem. Soc., Chem. Commun.* **1992**, 1386.

(3) Rovira, C.; Whangbo, M.-H. *Inorg. Chem.* **1993**, *32*, 4094.

(4) Wypych, F.; Weber, Th.; Prins, R. *Surf. Sci.* **1997**, *380*, L474.

(5) Brown, B. E. *Acta Crystallogr.* **1966**, *20*, 268.

(6) Wypych, F.; Prins, R.; Solenthaler, C.; Weber, Th., to be published.

S0897-4756(97)00402-X CCC: $15.00
Published on Web 02/07/1998

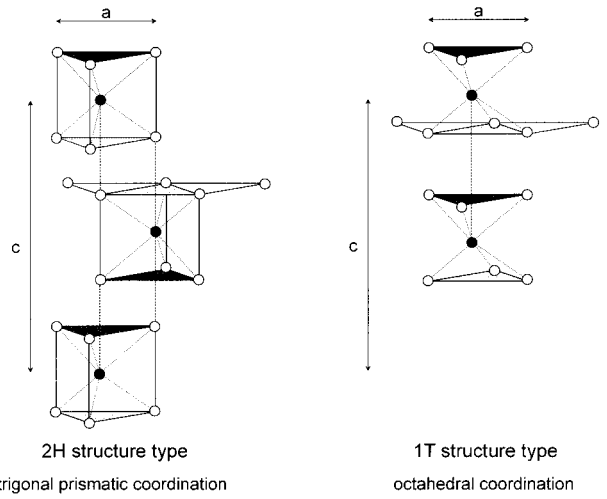

Figure 1. Schematic presentation of a 2H and a 1T type bulk structure with regular coordination of the metal centers.

compounds, with Li^+ concentrations ranging from $z \approx 0$ to $z = 1$, can be obtained by high-temperature reactions between Li_2S, Mo and S. In this case compounds with triclinic or monoclinic structures of the type $2a \times 2a$ form.[8] If the preparation is done by reaction between 2H−MoS_2 and *n*-butyllithium, the $2a \times 2a$ superstructure forms only when the Li^+ concentration exceeds $z = 1.3$. A subsequent reaction of Li_zMoS_2 with water in an ultrasonic bath leads to a suspension consisting of MoS_2 single layers (exfoliation).[9,10]

Detailed investigations of such suspensions containing MoS_2 single layers[10−12] confirmed that the coordination of molybdenum changes from a trigonal prismatic to a distorted octahedral coordination mode (2H → 1T-type phase transition) if the stacked MoS_2 layers (as in 2H−MoS_2) are converted into a set of MoS_2 single layers. STM measurements on thin films of MoS_2 prepared from such suspensions on graphite showed that the superstructure of an MoS_2 single layer corresponds to an $a \times 2a$-structure type[13,14] instead of $2a \times 2a$ as previously reported.[11] Similar superstructure types are also observed in nanocomposites, obtained by intercalating organic macromolecules between the layers of 2H−MoS_2.[15−21] Whereas the intercalation of organic macromolecules between the layers of 2H−MoS_2 leads to a material with metallic properties (1T type), reorganization to the 2H structure type takes place upon deintercalation.

This paper discusses the surface structure of the metastable compound 1T-MoS_2, as determined by STM, and compares it with the surface structures of potassium intercalated MoS_2-type compounds and MoS_2 single layers.

Experimental Section

1T-MoS_2 was prepared from K_2MoO_4 by sulfidation ($K_2MoO_4 + 4\ H_2S \rightarrow K_2MoS_4 + 4\ H_2O$), subsequent reduction ($2K_2MoS_4 + 3H_2 \rightarrow 2K_zMoS_2 + 2yK^0 + K_2S + 3H_2S$, $y < 1$, $z = 1 - y$), hydration ($K_zMoS_2 + (n + y)H_2O \rightarrow K_x(H_2O)_yMoS_2 + n/2H_2 + n$KOH, $x = z - n$), and oxidation. A detailed description of the preparation of $K_x(H_2O)_yMoS_2$, i.e., the first three steps in the sequence mentioned above, can be found in ref 4. Preliminary information about X-ray single-crystal analysis[22] showed that the structure of K_zMoS_2 is triclinic (space group *P*1, lattice parameters: $a = 0.660 \pm 0.01$ nm, $b = 0.661 \pm 0.01$ nm, $c = 0.799 \pm 0.03°$, $\alpha = 76.23 \pm 0.2°$, $\beta = 88.3 \pm 0.3°$, $\gamma = 60.26 \pm 0.3°$) and corresponds approximately to an $2a \times 2a$ superstructure of 2H−MoS_2. Therefore, the local coordination of both molybdenum and potassium is distorted octahedral. Hydration of the K^+ cations in K_zMoS_2 with H_2O, i.e., the formation of $K_x(H_2O)_yMoS_2$ ($x \approx 0.3$), occurs at the same time as a partial oxidation leading to the $a \times a\sqrt{3}$ superstructure of the hydrated phase.[2,4,23]

Oxidation of $K_x(H_2O)_yMoS_2$ to 1T-MoS_2 was done with a saturated solution of I_2 in CH_3CN. Depending on the reaction time, products with different surface structures can be obtained. Whereas the formation of 1T-MoS_2 with the expected $a\sqrt{3} \times a\sqrt{3}$ superstructure requires a reaction time of at least 60 min, an incomplete oxidation product with an $a \times 2a$-type superstructure can be obtained after an oxidation time of 15 min ($K_x(H_2O)_yMoS_2$, $\times < 0.3$). If a solution of $K_2Cr_2O_7$ in H_2SO_4[2] is used for the oxidation of $K_x(H_2O)_yMoS_2$, the surface of the formed 1T-MoS_2 is substantially destroyed. Under these conditions, sulfur ligands of the MoS_2 phase are protonated and released in the form of H_2S.

For the STM measurements single crystals of 1T-MoS_2 and the incomplete oxidation product were fixed on a metal sample holder using conductive silver paint (Drs. Bender and Hobein AG, Zurich). Immediately thereafter, the samples were measured with a Digital Instruments Nanoscope II scanning tunneling microscope under ambient conditions using commercially available 0.25 mm $Pt_{0.8}Ir_{0.2}$ tips. The tips were used as purchased or were resharpened. All the experiments were performed in the constant current mode with a negative bias voltage.

Results and Discussion

Oxidation of $K_x(H_2O)_yMoS_2$ ($x \approx 0.3$) with I_2/CH_3CN leads to MoS_2-type compounds with different surface structures, i.e., to MoS_2-type materials with an $a \times 2a$ and an $a\sqrt{3} \times a\sqrt{3}$-type superstructure after 15 and 60 min of oxidation, respectively. We will start by describing the STM images obtained from the incomplete oxidation product.

The STM image shown in Figure 2 represents the surface of the incomplete oxidation product of $K_x(H_2O)_yMoS_2$ ($x < 0.3$) in the region of 1.6 × 1.6 nm. The surface structure of this compound resembles the $2a \times$

(7) Chrissafis, K.; Zamani, M.; Kambas, K.; Stoemenos, J.; Economou, N. A.; Samaras, I.; Julien, C. *Mater. Sci. Eng.* **1986**, *B3*, 145.
(8) Mulhern, P. J. *Can. J. Phys.* **1989**, *67*, 1049.
(9) Joensen, P.; Frindt, R. F.; Morrison, S. R. *Mater. Res. Bull.* **1986**, *21*, 457.
(10) Joensen, P.; Crozier, E. D.; Alberding, N.; Frindt, R. F. *J. Phys. C* **1987**, *20*, 4043.
(11) Yang, D.; Jimenez Sandoval, S.; Divigalpitiya, W. M. R.; Irwin, J. C.; Frindt, R. F. *Phys. Rev. B* **1991**, *43*, 12053.
(12) Jimenez Sandoval, S.; Yang, D.; Frindt, R. F.; Inwin, J. C. *Phys. Rev. B* **1991**, *44*, 3955.
(13) Qin, X. R.; Yang, D.; Frindt, R. F.; Irwin, J. C. *Phys. Rev. B* **1991**, *44*, 3490.
(14) Qin, X. R.; Yang, D.; Frindt, R. F.; Inwin, J. C. *Ultramicroscopy* **1992**, *42−44*, 630.
(15) Ruiz-Hitzky, E.; Jimenes, R, Casal, B.; Manriquez, V.; Santa Ana, A, Gonzalez, G.; *Adv. Mater.* **1993**, *5*, 738.
(16) Kanatzidis, M. G.; Bissessur, R.; De Groot, D. C.; Schindler, J. L.; Kannewurf, C. R. *Chem. Mater.* **1993**, *5*, 595.
(17) Bissessur, R.; Kanatzidis, M. G.; Schindler, J. L.; Kannewurf, C. R. *J. Chem. Soc., Chem. Commun.* **1993**, 1582.
(18) Bissessur, R.; Schindler, J. L.; Kannewurf, C. R.; Kanatzidis, M. *Mol. Cryst. Liq.* Cryst. **1994**, *245*, 249.
(19) Wang, L.; Schindler, J.; Thomas, J. A.; Kannewurf, C. R.; Kanatzidis, M. G. *Chem. Mater.* **1995**, *7*, 1753.
(20) Zhou, X.; Yang, D.; Frindt, R. F. *J. Phys. Chem. Solids* **1996**, *57*, 1137.
(21) Lemmon, J. P.; Lerner, M. M. *Chem. Mater.* **1994**, *6*, 207.
(22) Wypych, F.; Prins, R.; Kronseder, C.; Nesper, R.; Weber, Th., to be published.

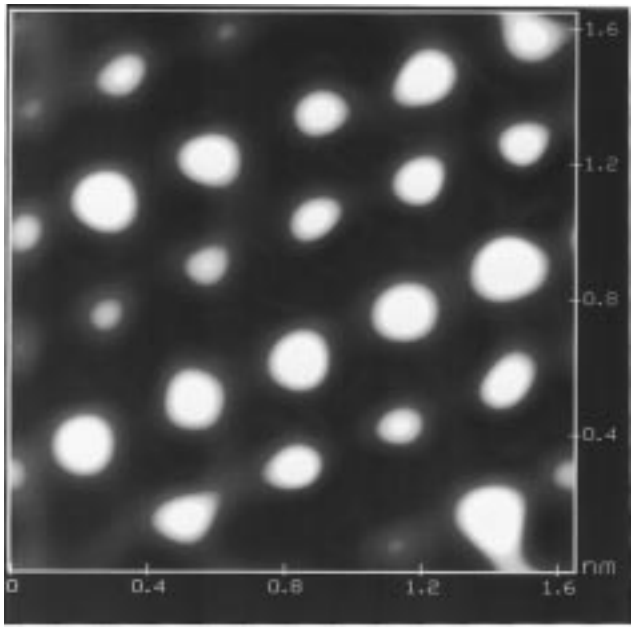

Figure 2. STM image of the incomplete oxidation product of $K_x(H_2O)_yMoS_2$, i.e., of $K_x(H_2O)_yMoS_2$, $x < 0.3$, in a region of 1.6×1.6 nm obtained with a bias voltage of -0.6 mV and an average current of 4.6 nA, after filtering.

a superstructure as observed in films of MoS_2 single layers on graphite[13,14] and consists of parallel chains of sulfur atoms. The sulfur atoms within one chain are displaced in the direction of the *c*-axis and occupy alternating positions above and below the (*a*,*b*) surface plane. The bright spots in the STM image shown in Figure 2 are due to the sulfur atoms at top positions.

Figure 3 shows the interpolated cross section along the chains (along the *a*-axis (Figure 3a)) and along the *b*-axis (Figure 3b) of the $2a \times a$ superlattice. The measured distance between sulfur atoms in a chain is 0.32 ± 0.01 nm (independent of their position with respect to the (*a*,*b*) plane). This value is in good agreement with the respective S−S distances in $K_x(H_2O)_y$-MoS_2 ($a = 0.324$ nm) and in 1T-MoS_2 ($a\sqrt{3} = 0.5594$, $a = 0.323$ nm). Determination of the distances between neighboring sulfur atoms located above and below the (*a*,*b*) plane on the basis of the STM data is impossible. Measurements in the projections along the $2a \times a$ superlattice showed that the average distances between sulfur atoms above and below the (*a*,*b*) plane is 0.31 ± 0.01 nm within a chain (Figure 2a) and 0.40 ± 0.01 nm between the chains. Due to the periodic displacement of the sulfur atoms above and below the (*a*,*b*) plane the distance between them should, however, be slightly larger.

These findings are complementary to the results of a structural study on single layers of MoS_2. Extended X-ray absorption fine structure (EXAFS) measurements of aqueous suspensions containing MoS_2 single layers revealed a serious distortion of these single layers with respect to bulk 2H−MoS_2. In addition to the characteristic Mo−Mo distance of 0.316 nm, Mo−Mo contributions at 0.28 and 0.38 nm were found.[10] Although the Mo−Mo distances cannot be compared directly with S−S distances, a displacement of Mo centers from their ideal crystallographic positions in 2H−MoS_2 will always lead to a displacement of sulfur ligands and to a

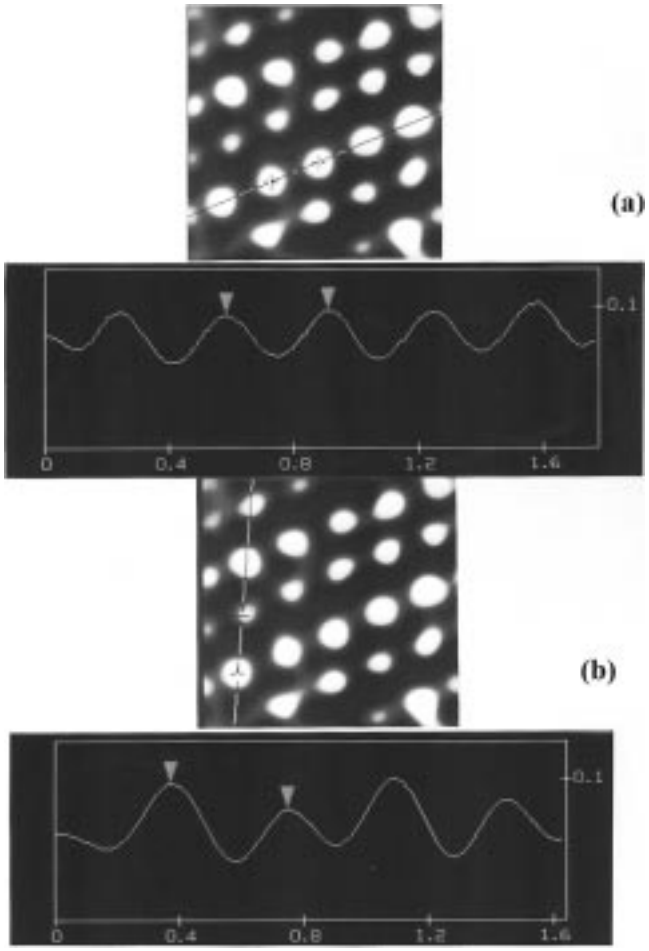

Figure 3. Interpolated cross section along the *a*-axis (a) and along the *b*-axis (b) of the STM image shown in Figure 2.

distortion of the local coordination environment of the Mo centers. On the basis of this consideration it is likely that the [MoS_6] octahedra in the incomplete oxidation product, i.e., in $K_x(H_2O)_yMoS_2$, $\times < 0.3$, are distorted in such a way that all six Mo−S distances are different and not only three as mentioned above. The lattice parameters of this compound, determined by means of STM measurements, are $a = 0.33 \pm 0.01$ nm, $b = 0.71 \pm 0.01$ nm, and $\gamma = 63 \pm 0.5°$ ($a \times 2a$). However, there is another possibility for describing the superlattice, namely, $a = 0.33 \pm 0.01$ nm, $b = 0.65 \pm 0.01$ nm, and $\gamma = 91 \pm 0.5°$ ($a \times a\sqrt{3}$). Both possibilities are shown schematically in Figure 4.

The structural distortion of MoS_2 single layers with respect to bulk 2H−MoS_2 corresponds with supported MoS_2-type hydrotreating catalysts. Coordination defects, as discussed in ref 24, as well as insufficient packing of MoS_2 layers, i.e., a significant decrease in the van der Waals interactions, lead to changes in the surface morphology and to a bending of MoS_2 slabs.[25] Both examples, i.e., the single layers and the MoS_2-type catalyst, show the structural flexibility of these compounds as well as the importance of van der Waals forces for the MoS_2 structure.

(23) Schöllhorn, R.; Kümpers, M.; Florin, D. *J. Less-Common. Met.* **1978**, *58*, 55.
(24) Weber, Th.; Muijsers, J. C.; van Wolput, J. H. M. C.; Verhagen, J. P. C.; Niemantsverdriet, J. W. *J. Phys. Chem.* **1996**, *100*, 14144.
(25) Muijsers, J. C.; Weber, Th.; van Hardeveld, R. M.; Zandbergen, H. W.; Niemantsverdriet, J. W. *J. Catal.* **1995**, *157*, 698.

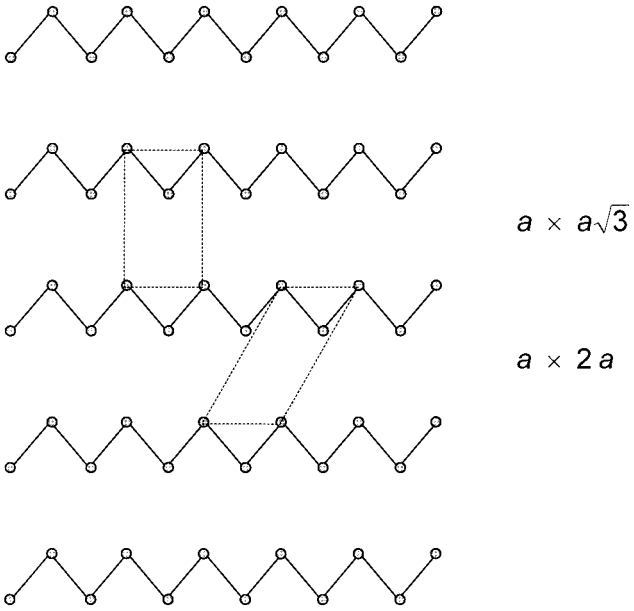

Figure 4. Formation of the $a \times a\sqrt{3}$ and $a \times 2a$ superstructures (schematically).

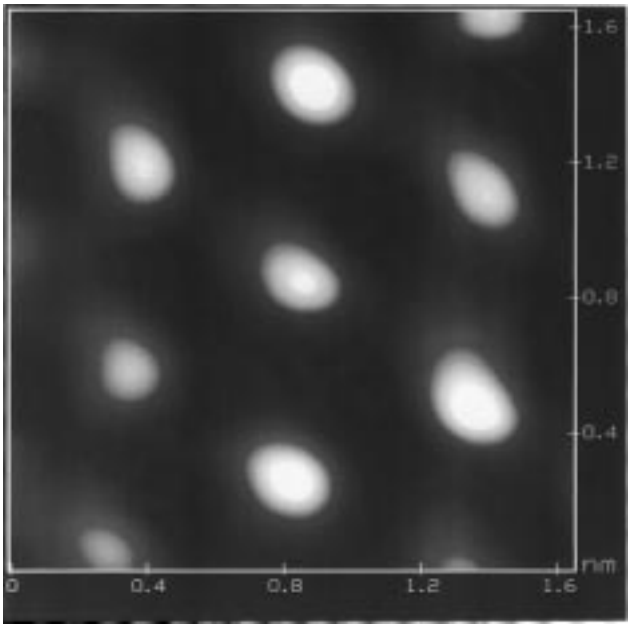

Figure 5. STM image of 1T-MoS_2 obtained with a bias voltage of −110.8 mV and an average current of 10.2 nA in a region of 1.6 × 1.6 nm after filtering.

Oxidation of $K_x(H_2O)_yMoS_2$ in an I_2/CH_3CN solution for 60 min or longer leads to the formation of 1T-MoS_2. The STM image shown in Figure 5 represents the surface of 1T-MoS_2 in the region 1.6 × 1.6 nm. The measurements are of such quality that the $a\sqrt{3} \times a\sqrt{3}$ superstructure can clearly be recognized. The lattice parameters as determined by STM, $a = 0.56 \pm 0.01$ nm and $\gamma = 120 \pm 0.5°$, are in perfect agreement with those determined by means of XRD and SAED measurements: $a = b = 0.559$ nm, $\gamma = 20°$.[2]

It is interesting that some of our STM measurements indicated an $a \times a\sqrt{3}$ superstructure instead of the expected $a\sqrt{3} \times a\sqrt{3}$ superstructure, whereas AFM measurements on films of MoS_2 single layers on mica gave evidence of the presence of an $a\sqrt{3} \times a\sqrt{3}$-type superstructure in some regions of the samples (cf. Figure 2a in ref 26). This shows that the actual type of structure not only is an intrinsic property of these phases but also depends on the external stabilization of the structural disorder. In the case of 1T-MoS_2, the observation of an $a \times a\sqrt{3}$ superstructure may be due to an incomplete oxidation of $K_x(H_2O)_yMoS_2$ (note that $a \times a\sqrt{3}$ is the expected superstructure for $K_x(H_2O)_y$-MoS_2[6]) or, more likely, to a film of water on some of the layers, as reported for the single layers of MoS_2 after exfoliation.[13,14,26] Here, a further distortion of the local coordination environment of Mo leading to the $a\sqrt{3} \times a\sqrt{3}$ superstructure is not necessary for effective stabilization of the phase. This effect of stabilization is crucial for understanding the structural chemical properties of these compounds and can be recognized during the whole oxidation sequence leading to 1T-MoS_2, i.e., K_zMoS_2, $z \approx 0.7$ ($2a \times 2a$) → $K_x(H_2O)_yMoS_2$, $x \approx 0.3$ ($a \times a\sqrt{3}$) → $K_x(H_2O)_yMoS_2$, $x < 0.3$ ($a \times 2a$) → 1T-MoS_2 ($a\sqrt{3} \times a\sqrt{3}$). The corresponding structure is stabilized by the intercalated cations or by H_2O which can be associated either with the intercalated cations (hydration) or with the surface of the sample.

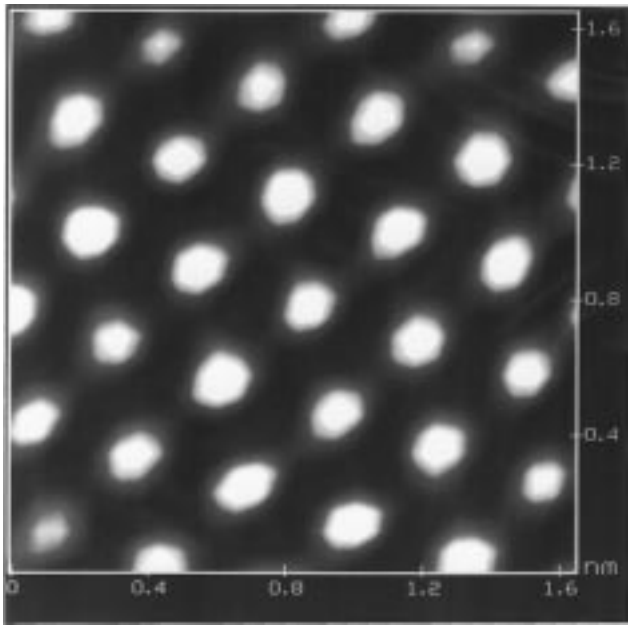

Figure 6. STM image of 1T-MoS_2 after thermal treatment in the DSC obtained with a bias voltage of −1847.2 mV and an average current of 2 mA in a region of 1.6 × 1.6 nm after filtering.

Long-term measurements of 1T-MoS_2 showed that the material is stable in air for about 5 days. Whereas the $a\sqrt{3} \times a\sqrt{3}$ superlattice was clearly visible during the first 3 days, it nearly disappeared after 5 days.

The STM image shown in Figure 6 was obtained after treating the 1T-MoS_2 crystal in the differential scanning calorimeter (DSC) at 300 °C (N_2 atmosphere, heating rate 2 °C/min). The DSC pattern shows an exothermic peak at ca. 100 °C that can be attributed to a 1T → 2H phase transition. After phase transition, the surface structure of the sample (Figure 6) is similar to that of restacked MoS_2 single layers or 2H−MoS_2 with a distorted surface.

(26) Schumacher, A.; Scandella, L.; Kruse, N.; Prins, R. *Surf. Sci.* **1993**, *289*, L595.

Conclusion

Oxidation of the ternary phase $K_x(H_2O)_yMoS_2$ with a solution of I_2 in CH_3CN leads to the formation of MoS_2-type phases with different surface structures.

After 15 min of oxidation, a phase with an $a \times 2a$ superstructure appears. After at least 60 min of oxidation, crystalline 1T-MoS_2, with the expected $a\sqrt{3} \times a\sqrt{3}$ surface structure, is formed. This compound is stable for a couple of days, whereas it converts to 2H−MoS_2 upon heating in an inert gas atmosphere. The 1T → 2H phase transition can be seen as an exothermic peak in the DSC and takes place at around 100 °C. STM images of the sample after thermal treatment are similar to those of samples consisting of restacked MoS_2 single layers or 2H−MoS_2 with a distorted surface.

The sequence in this distortion can be followed easily by observing the K_xMoS_2 hydration and oxidation sequence, i.e., $K_zMoS_2 \rightarrow K_x(H_2O)_yMoS_2 \rightarrow$ 1T-MoS_2. The type of distortion in the respective compound is stabilized by intercalated cations. Their presence enables the change in the local coordination geometry of the Mo centers from trigonal prismatic to distorted octahedral. In the case of the MoS_2 single layers as prepared by exfoliation with *n*-butyllithium, stabilization is achieved by a bilayer of water or by hydrated Li^+ cations associated with the MoS_2 layers, respectively.

Acknowledgment. F.W. expresses his thanks to the Department of Chemistry, Federal University of Paraná, for granting him a leave of absence.

CM970402E